International Applied Mechanics, Vol. 46, No. 2, 2010

APPROXIMATE DESCRIPTION OF THE INELASTIC DEFORMATION OF AN ISOTROPIC MATERIAL WITH ALLOWANCE FOR THE STRESS MODE

M. E. Babeshko, Yu. N. Shevchenko, and N. N. Tormakhov

The elastoplastic deformation of an isotropic material is described using constitutive equations and allowing for the stress mode. The equations include two nonlinear functions that relate the first and second invariants of the stress and linear-strain tensors to the stress mode angle. It is proposed to use a linear rather than nonlinear relationship between the first invariants of the tensors. This simplification is validated by comparing calculated and experimental strains under loading with constant and variable stress mode angle

Keywords: isotropic material, elastoplastic deformation, constitutive equations, stress mode angle

Introduction. Constitutive equations describing the elastoplastic deformation of isotropic materials along small-curvature paths and allowing for the stress mode were proposed in [10, 11]. These equations relate the stress components and the linear strain components and can be used both at small and large strains. It was assumed that stress deviators and differentials of plastic strains are coaxial. The equations contain two nonlinear functions that depend on a stress mode parameter. For this parameter, the stress mode angle was used in [3]. One function relates the mean stress and strain and the stress mode angle, while the other function relates the intensities of tangential stresses and shear strains and the stress mode angle. These functions are determined from tests on tubular specimens under tension and internal pressure increased proportionally, i.e., at several constant stress mode angles. When these functions are assumed independent of the stress mode angle and determined from uniaxial-tension tests, the above equations transform into the standard equations of the theory of deformation along small-curvature paths [2, 4, 5, 13], which are widely used to solve boundary-value problems [6–9, etc.].

The assumptions underlying the constitutive equations were validated in [10–12] against the data of tests on tubular specimens subject to tension and internal pressure. The specimens were made of Kh18N10T steel and preliminarily annealed.

An approximate method to calculate the above functions from test data for stress mode angles $\omega_\sigma = 0, \pi/6, \pi/3$ (base functions) was proposed in [1]. For intermediate values of ω_σ, linear interpolation was used. The base functions and the algorithm developed in [1] were used to analyze several deformation processes for tubular specimens for different stress mode angles. The calculated strains were in satisfactory agreement with experimental data.

In support of [10–12] and in contrast to [1], the present paper uses a more simple approximate approach to describe the inelastic deformation of isotropic materials with allowance for the stress mode. This approach assumes that the relationship between the mean stress and the mean strain is independent of the stress mode, while the relationship between the intensities of tangential stresses and shear strains is dependent on the stress mode. The approach will be tested against specific examples.

1. Constitutive Equations. To formulate the constitutive equations, we will divide the loading process into small steps. At the *N*th step, the components of the stress σ_{ij} and strain ε_{ij} tensors are related by

$$\sigma_{ij} = \frac{2G}{1-2\nu}\left[(1-2\nu)\varepsilon_{ij} + 3\nu\varepsilon_0\delta_{ij}\right] - 2G\varepsilon_{ij}^{(p)}, \tag{1.1}$$

S. P. Timoshenko Institute of Mechanics, National Academy of Sciences of Ukraine, 3 Nesterov St., Kyiv, Ukraine 03057, e-mail: plast@inmech.kiev.ua. Translated from Prikladnaya Mekhanika, Vol. 46, No. 2, pp. 24–34, February 2010. Original article submitted February 19, 2009.

where G and ν are the shear modulus and Poisson's ratio,

$$\varepsilon_0 = \varepsilon_{ij}\delta_{ij} / 3, \tag{1.2}$$

δ_{ij} is the Kronecker delta, $\delta_{ij} = 1$ if $i = j$ and $\delta_{ij} = 0$ if $i \neq j$.

Assume that the components of the strain tensor include elastic $\varepsilon_{ij}^{(e)}$ and plastic $\varepsilon_{ij}^{(p)}$ components:

$$\varepsilon_{ij} = \varepsilon_{ij}^{(e)} + \varepsilon_{ij}^{(p)}. \tag{1.3}$$

The elastic components obey Hooke's law.

The plastic components are determined as the sum of their increments $\Delta\varepsilon_{ij}^{(p)}$ at the end of the Nth step:

$$\varepsilon_{ij}^{(p)} = \sum_{k=1}^{N} \Delta_k \varepsilon_{ij}^{(p)}. \tag{1.4}$$

Assume that the mean stress

$$\sigma_0 = \sigma_{ij}\delta_{ij} / 3 \tag{1.5}$$

and the mean strain (1.2) are related linearly:

$$\varepsilon_0 = \frac{\sigma_0}{K}, \quad K = \frac{2G(1+\nu)}{1-2\nu}. \tag{1.6}$$

Due to (1.6), the plastic components of the strain tensor are equal to the components of the plastic-strain deviator ($\varepsilon_{ij}^{(p)} = e_{ij}^{(p)}$), and the increments $\Delta_k \varepsilon_{ij}^{(p)}$ at the kth step of loading are given by

$$\Delta_k \varepsilon_{ij}^{(p)} = \left\langle \frac{s_{ij}}{S} \right\rangle_k \Delta_k \Gamma^{(p)}, \tag{1.7}$$

where

$$s_{ij} = \sigma_{ij} - \sigma_0 \delta_{ij}, \tag{1.8}$$

S is the intensity of tangential stresses,

$$S = \left(\frac{1}{2} s_{ij} s_{ij} \right)^{1/2}, \tag{1.9}$$

$\Delta_k \Gamma^{(p)}$ is the increment of the intensity of plastic shear strains at the kth step,

$$\Gamma^{(p)} = \sum_{k=1}^{N} \Delta_k \Gamma^{(p)}. \tag{1.10}$$

The angular brackets in (1.7) denote averaging.

To determine $\Delta_k \Gamma^{(p)}$, we assume that

$$S = F_2(\Gamma, \omega_\sigma), \tag{1.11}$$

where

$$\Gamma = \left(\frac{1}{2} e_{ij} e_{ij} \right)^{1/2} \tag{1.12}$$

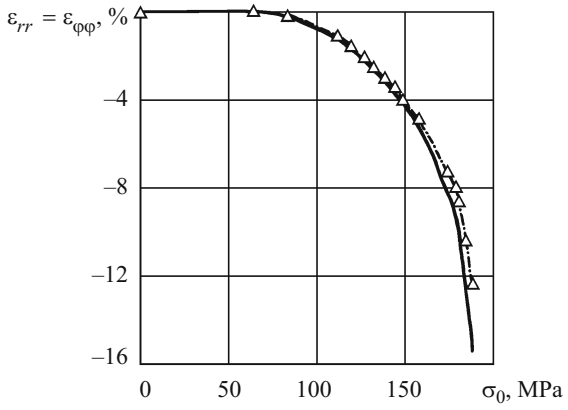

Fig. 1

is the intensity of shear strains,

$$e_{ij} = \varepsilon_{ij} - \varepsilon_0 \delta_{ij}, \tag{1.13}$$

$$\omega_\sigma = \frac{1}{3}\arccos\left[-\frac{3\sqrt{3}}{2}\frac{I_3(D_\sigma)}{S^3}\right] \quad (0 \le \omega_\sigma \le \pi/3) \tag{1.14}$$

is the stress mode angle [3, 10], $I_3(D_\sigma)$ is the third invariant of the stress deviator equal to its determinant:

$$I_3(D_\sigma) = |s_{ij}|. \tag{1.15}$$

The stress mode angle ω_σ is determined in terms of the components of the stress deviator, unlike the Lode parameter, which is determined in terms of the principal stresses. This angle is related to the Lode parameter μ_σ in a simple manner [3]: $\omega_\sigma = \pi/3$, $\mu_\sigma = -1$ in tension; $\omega_\sigma = 0$, $\mu_\sigma = 1$ if the principal stresses are equal ($\sigma_1 = \sigma_2$); $\omega_\sigma = \pi/6$, $\mu_\sigma = 0$ in shear or if $2\sigma_1 = \sigma_2$.

To individualize the function F_2 (1.11), we will use, as in [1], data of base tests on tubular specimens proportionally loaded by a tensile axial force and internal pressure at several constant values of ω_σ as well as the assumption

$$\Gamma = \frac{S}{2G} + \Gamma^{(p)}. \tag{1.16}$$

Thus, the constitutive equations describing the deformation of isotropic materials include (1.1), (1.6), (1.7), and (1.11). These equations are distinguished from those in [10–12] by the assumption (1.6) because it was assumed in [10–12] that the relationship between the mean stress σ_0 and the mean strain ε_0 is nonlinear and dependent on the stress mode:

$$\sigma_0 = F_1(\varepsilon_0, \omega_\sigma). \tag{1.17}$$

To individualize function (1.17), we will use the results of the base tests conducted to find the function F_2 (1.11).

2. Calculation of Base Functions. As noted above, function (1.11) should be calculated from tests on tubular specimens under tension and internal pressure at $\omega_\sigma = 0, \pi/6, \pi/3$. Next, these values are used to analyze the deformation of tubular specimens at $0 \le \omega_\sigma \le \pi/3$ and to solve boundary-value problems with allowance for the stress mode. It is difficult to determine the base functions because in addition to the stresses σ_{zz} and $\sigma_{\varphi\varphi}$ and the strains ε_{zz} and $\varepsilon_{\varphi\varphi}$, which can be found experimentally, it is necessary to find the radial strain ε_{rr} that cannot be measured directly.

Unlike [1], we will approximately calculate the radial strain from an expression derived from (1.6):

$$\varepsilon_{rr} = \frac{3\sigma_0(1-2\nu)}{2G(1+\nu)} - \varepsilon_{zz} - \varepsilon_{\varphi\varphi}. \tag{2.1}$$

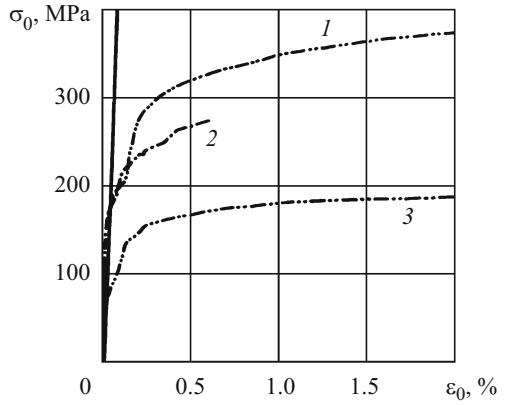

Fig. 2

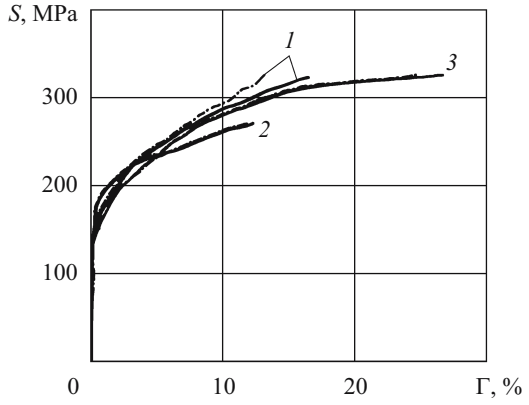

Fig. 3

In using formulas (1.6) and (2.1), it is assumed that the mean plastic strain is zero ($\varepsilon_0^{(p)} = 0$). As shown in [1, 11], $\varepsilon_0^{(p)} \cdot 10^2 = 2$ after the tension of a tubular specimen is completed [11], i.e., $\varepsilon_0^{(p)} = 0$ in this process. Let us evaluate the disagreement between the values of strain $\varepsilon_{rr} = \varepsilon_{\varphi\varphi}$ predicted by formula (2.1) and measured in tests.

Figure 1 shows the strain $\varepsilon_{rr} = \varepsilon_{\varphi\varphi}$ versus the mean stress σ_0. Here the solid line corresponds to formula (2.1), the dashed line to the approach [1], and the triangles to experiment. As is seen, values $\varepsilon_{rr} = \varepsilon_{\varphi\varphi}$ calculated by the approach [1] are in agreement with the experimental data. The relative error of maximum strain $\varepsilon_{rr} = \varepsilon_{\varphi\varphi}$ calculated by (2.1) is $\delta = 16\%$, where $\delta = \left| \dfrac{\varepsilon_{\text{calc}} - \varepsilon_{\text{exp}}}{\varepsilon_{\text{exp}}} \right| \cdot 100$, $\varepsilon_{\text{calc}}$ and ε_{exp} are the calculated and experimental strains, respectively.

Let us analyze the difference between the base functions F_1 (1.17), Fig. 2, and F_2 (1.11), Fig. 3, calculated for $\omega_\sigma = 0$, $\pi/6$, and $\pi/3$, by our method and the method of [1]. In Figs. 2 and 3, as in Fig. 1, the solid lines correspond to formula (2.1), the dashed lines to the approach [1], and curves *1*, *2*, and *3* correspond to $\omega_\sigma = 0, \pi/6, \pi/3$, respectively.

The solid line in Fig. 2 corresponding to (1.6) both quantitatively and qualitatively differs from dashed curves *1*, *2*, *3* corresponding to (1.17). Figure 2 also demonstrates that the base function F_1 (1.17) for $\varepsilon_0 \cdot 10^2 \geq 0.2$ is strongly dependent on ω_σ. For example, the values of σ_0 corresponding to the same value of ε_0 on dashed curves *1* and *3* differ twofold approximately. Dashed curve *2* in Fig. 2 corresponding to $\omega_\sigma = \pi/6$ does not pass midway between curves *1* ($\omega_\sigma = 0$) and *3* ($\omega_\sigma = \pi/3$). This means that with few base curves, the linear interpolation with respect to ω_σ may produce a considerable error.

Figure 3 demonstrates that the base function F_2 (1.11) calculated by [1] and (2.1) differ only quantitatively, the difference being $\delta = 23\%$ (curve *1*) at the same intensity of tangential stresses.

Calculations shows that at the end of the processes being considered, the intensity of shear strains is approximately an order of magnitude greater than the mean strain. This makes it possible to assume that dependence of the function F_1 (1.17) on the stress mode have a weaker effect on the calculated strains than the same dependence of the function F_2 (1.11). Therefore, it seems to be expedient to use relation (1.6) instead of (1.17), avoiding the interpolation of the function F_1 at intermediate stress mode angles.

3. Approximate Analysis of the Deformation of a Tubular Specimen. We assume that the way a tubular specimen is loaded by axial force and internal pressure is known. Let us set up an algorithm to calculate the strains in the specimen using the constitutive equations (1.1), (1.6), (1.7), and (1.11), allowing for the dependence of the function F_2 (1.11) on the stress mode, and replacing the function F_1 (1.17) by (1.6). Note that this algorithm is somewhat simpler than that in [1]. Let us divide the loading process into steps and assume that the stress components and base function F_2 (1.11) for $\omega_\sigma = 0, \pi/6, \pi/3$ are known at each step. First, we use the values of the stresses and formulas (1.5), (1.8), (1.9), and (1.14) to calculate σ_0, S, and ω_σ. Then, we interpolate the values of F_2 at $\omega_\sigma = 0, \pi/6, \pi/3$ to find F_2 for a given value of ω_σ. Next, we use this function and the intensity of tangential stresses S (1.9) at the end and beginning of the current step of loading to determine the intensity of shear strains Γ. After that, we use formula (1.16) to calculate the intensity of plastic shear strains $\Gamma^{(p)}$ and the increment $\Delta_k \Gamma^{(p)}$:

TABLE 1

σ_{zz}, MPa	$\varepsilon_{zz} \cdot 10^2$				$\varepsilon_{rr} \cdot 10^2 = \varepsilon_{\varphi\varphi} \cdot 10^2$			
	exp.	1	2	3	exp.	1	2	3
192	0.1	0.1	0.1	0.1	0	0	0	0
251	0.6	0.6	0.6	0.5	–0.2	–0.2	–0.2	–0.2
337	2.5	2.5	2.5	2.4	–1.1	–1.1	–1.2	–1.2
359	3.5	3.5	3.5	3.4	–1.6	–1.6	–1.7	–1.7
382	4.5	4.5	4.5	4.4	–2.1	–2.1	–2.2	–2.2
397	5.5	5.5	5.5	5.4	–2.5	–2.6	–2.7	–2.6
417	6.5	6.5	6.5	6.4	–3.0	–3.0	–3.2	–3.1
435	7.5	7.5	7.5	7.3	–3.4	–3.4	–3.7	–3.6
447	8.5	8.5	8.5	8.4	–4.0	–3.9	–4.2	–4.1
474	10.5	10.5	10.5	10.3	–4.8	–4.8	–5.2	–5.1
523	16.5	16.5	16.5	15.9	–7.3	–7.3	–8.2	–7.9
537	18.5	18.5	18.5	17.7	–8.0	–8.0	–9.2	–8.8
543	20.0	20.0	20.0	19.1	–8.6	–8.6	–9.9	–9.5
554	25.0	25.0	25.0	23.6	–10.4	–10.3	–12.4	–11.7
566	31.0	31.0	31.0	28.9	–12.4	–12.4	–15.4	–14.4

$$\Delta_k \Gamma^{(\mathrm{p})} = \Gamma_k^{(\mathrm{p})} - \Gamma_{k-1}^{(\mathrm{p})} = \left(\Gamma - \frac{S}{2G}\right)_k - \left(\Gamma - \frac{S}{2G}\right)_{k-1}, \tag{3.1}$$

where k and $k-1$ are the numbers of the current and previous steps of loading. Now, we determine the increments of the plastic strain components:

$$\Delta_k \varepsilon_{zz}^{(\mathrm{p})} = \left\langle \frac{\sigma_{zz} - \sigma_0}{S} \right\rangle_k \Delta_k \Gamma^{(\mathrm{p})} \qquad (z, \varphi),$$

$$\Delta_k \varepsilon_{rr}^{(\mathrm{p})} = \left\langle \frac{-\sigma_0}{S} \right\rangle_k \Delta_k \Gamma^{(\mathrm{p})} \tag{3.2}$$

and the plastic components themselves (1.4) to find the elastic strain components by the formulas

$$\varepsilon_{zz}^{(\mathrm{e})} = \frac{\sigma_{zz} - \nu\sigma_{\varphi\varphi}}{E} \quad (z, \varphi),$$

TABLE 2

σ_{zz}, MPa	$\sigma_{\varphi\varphi}$, MPa	$\varepsilon_{zz} \cdot 10^2$				$\varepsilon_{\varphi\varphi} \cdot 10^2$			
		exp.	1	2	3	exp.	1	2	3
252	254	0.28	0.16	0.16	0.31	0	0.17	0.17	0.32
279	282	0.45	0.28	0.28	0.61	0.05	0.29	0.28	0.63
304	313	0.81	0.65	0.64	0.91	0.50	0.68	0.68	0.96
327	335	1.08	0.96	0.95	1.15	0.88	1.01	1.01	1.22
366	398	1.72	1.74	1.70	2.18	1.88	1.94	1.91	2.44
401	429	2.59	2.55	2.54	2.98	2.90	2.94	2.95	3.43
418	440	3.03	3.08	3.01	3.31	3.49	3.55	3.51	3.83
436	455	3.54	3.53	3.51	3.87	4.06	4.06	4.08	4.47
450	467	3.93	3.94	3.92	4.31	4.53	4.52	4.54	4.96
470	483	4.62	4.70	4.67	4.98	5.41	5.35	5.37	5.70
482	496	5.03	5.15	5.12	5.65	5.95	5.83	5.86	6.43
492	505	5.42	5.58	5.54	6.19	6.43	6.28	6.32	7.02
507	518	6.43	6.57	6.53	6.98	7.47	7.33	7.37	7.86
521	526	6.84	6.98	6.93	7.55	7.88	7.75	7.79	8.46
535	533	7.31	7.45	7.40	8.27	8.35	8.22	8.26	9.18
551	543	8.17	8.39	8.35	9.96	9.44	9.14	9.18	10.82
555	548	8.42	8.61	8.57	10.96	9.55	9.36	9.39	11.78
562	555	8.79	9.03	8.99	12.50	10.01	9.77	9.80	13.27
565	559	9.05	9.28	9.25	13.37	10.24	10.02	10.05	14.10

TABLE 3

σ_{zz}, MPa	$\sigma_{\varphi\varphi}$, MPa	$\varepsilon_{\varphi\varphi} \cdot 10^2$			
		exp.	1	2	3
167	334	0.36	0.35	0.35	1.21
194	387	1.11	1.09	1.11	2.09
216	431	2.64	2.58	2.61	3.55
232	464	4.68	4.57	4.64	4.07
233	466	5.31	5.19	5.27	4.98
238	475	5.86	5.73	5.82	5.31
241	481	6.68	6.54	6.63	5.54
247	494	7.62	7.42	7.55	6.05
250	499	8.04	7.83	7.98	6.28
253	506	8.69	8.44	8.60	6.61
257	514	9.54	9.32	9.46	7.10
260	519	10.03	9.81	9.95	7.42
263	526	10.61	10.34	10.52	7.76
264	529	10.85	10.57	10.74	7.93
268	536	11.88	11.56	11.78	8.29
272	544	12.67	12.30	12.55	8.75

$$\varepsilon_{rr}^{(e)} = -\frac{\nu(\sigma_{zz} + \sigma_{\varphi\varphi})}{E}, \tag{3.3}$$

where $E = 2G(1+\nu)$ is the elastic modulus. Finally, the strain components are determined as

$$\varepsilon_{zz} = \varepsilon_{zz}^{(e)} + \varepsilon_{zz}^{(p)} \quad (z, \varphi, r). \tag{3.4}$$

Thus, the above algorithm allows approximate calculation of the components of the strain tensor for a tubular specimen under loading of given type assuming that only the function F_2 (1.11) is dependent on the stress mode. If the function F_2 (1.11) is considered independent of the stress mode and equal to the base function at $\omega_\sigma = \pi/3$ (i.e., when the specimen is subject to uniaxial tension), then this algorithm may be used to determine the components of the strain tensor based on the theory of deformation along small-curvature paths [4, 5].

4. Numerical Results. Let us compare data for tubular specimens under tension and internal pressure obtained in the tests [11] and calculated:

(i) considering that the functions F_1 (1.17) and F_2 (1.11) depend on the stress mode, as in [1];

TABLE 4

σ_{zz}, MPa	$\sigma_{\varphi\varphi}$, MPa	$\varepsilon_{zz} \cdot 10^2$	$\varepsilon_{\varphi\varphi} \cdot 10^2$	ω_σ, rad
149	296	0	0.28	0.52
177	354	0	0.62	0.52
200	399	0	0.96	0.52
230	458	0	3.00	0.52
235	467	0	5.07	0.52
244	485	0	5.78	0.52
249	498	0	6.06	0.52
354	490	0	7.01	0.27
381	480	0.2	7.23	0.20
470	478	0.43	7.86	0.02
495	478	0.74	8.40	0.03
522	478	1.24	9.01	0.08
547	478	1.87	9.71	0.12
582	478	2.73	10.43	0.17
607	478	4.01	11.21	0.20
619	479	5.15	11.88	0.22

(ii) considering that only the function F_2 (1.11) depends on the stress mode and using the linear relation (1.6);

(iii) disregarding the stress mode and using the theory of deformation along small-curvature paths.

The algorithm outlined in [1] was used in case (i) and the algorithm outlined in Sec. 3 was used in cases (ii) and (iii).

Table 1 summarizes the experimental data [11] and calculated results for a tubular specimen under tension ($\omega_\sigma = \pi / 3$).

The first column contains the values of the axial stress and the other columns contain experimental ("exp.") and calculated (1, 2, 3 correspond to cases (i), (ii), (iii)) values of strains.

As is seen, the results obtained in case (i) differ from the experimental values by less than $\delta = 0.1\%$. In case (ii), the calculated maximum axial strains agree with the experimental values and the maximum hoop strains exceed the experimental values by 24%. In case (iii), the calculated maximum axial strains are less than the experimental values by 6% and the hoop strains exceed the experimental values by 16%. Note that all the calculated strains that are less than 10% differ from the experimental values by no more than $\delta = 10\%$.

Table 2 summarizes the experimental data [11] and calculated results for a tubular specimen under tension and internal pressure ($\omega_\sigma \approx 0$).

The first two columns contain stresses and the other columns strains, the notation being the same as in Table 1.

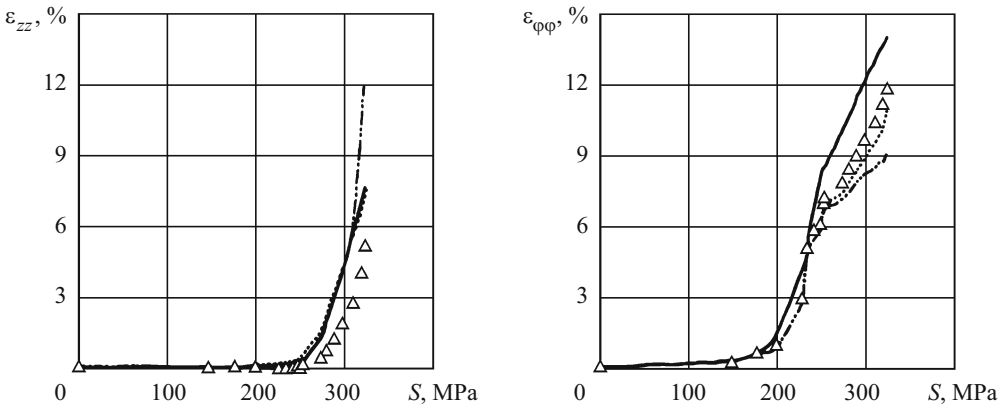

a *b*

Fig. 4

As is seen, in cases (i) and (ii), the calculated values differ from each other in the third decimal place and agree well with experimental data (the difference is less than $\delta = 2\%$ at the end of the process). In case (iii), the calculated strains that are less than 7.5% differ from the experimental values by less than $\delta = 10\%$, this difference reaching $\delta = 40\%$ at the end of the process.

Table 3 summarizes the experimental data [11] and calculated results for a tubular specimen under tension and internal pressure ($\omega_\sigma = \pi / 6$), the notation being the same.

Since the experimental and calculated axial strains are less than 0.2%, they are omitted in Table 3. In cases (i) and (ii), the calculated hoop strains differ from each other by less than $\delta = 1\%$ and agree well with the experimental values (the difference is less than 3%). In case (iii), the calculated hoop strains that are less than 7% differ from the experimental data by 10–12%, this difference reaching $\delta = 30\%$ at the end of the process.

Note that the stress mode angle in the above processes was kept constant, making it unnecessary to interpolate the base functions with respect to this parameter.

Let the stress mode angle change from step to step. In this case, interpolation is necessary. Table 4 summarizes experimental values of the axial and hoop stresses and strains [11]. The corresponding stress mode angles are given in the last column.

Figure 4 shows the calculated and experimental axial (Fig. 4*a*) and hoop (Fig. 4*b*) strains as functions of the intensity of tangential stresses. Cases (i), (ii), and (iii) are represented by solid, dotted, and dashed lines, respectively, while the experimental values are shown by triangles.

As is seen, when $S \le 250$ MPa and $\Gamma \cdot 10^2 \le 7.5$, the calculated values are in good agreement with the experimental data, but the difference increases with the load. At the end of the process, the calculated hoop strains are in better agreement with the experimental data than the axial strains, which are approximately 60% less than the hoop strains.

The results obtained in case (i) are in better agreement with the experimental data than the other results. The results obtained in case (ii) are slightly worse agreement with the experimental data than in case (i) but in better agreement than in case (iii). The difference of axial and hoop strains from the experimental data is 40 and 15%, respectively. In case (iii), the calculated axial and hoop strains differ from the experimental data by 50 and 20%, respectively.

Thus, the maximum calculated strains differ from the experimental data by less than 15% in cases (i) and (ii) and by 40% in case (iii). The less the calculated strain, the greater the difference in all cases. The maximum calculated strains can differ from the experimental data by 40% in cases (i) and (ii) and by more than 100% in case (iii). When the stress mode angle changes substantially during loading, the difference between calculated and experimental strains in cases (i) and (ii) can be decreased by increasing the number of given values of the base functions.

Conclusions. We have outlined an approximate approach to the numerical analysis of the elastic deformation of isotropic materials with allowance for the stress mode. This approach, which appears to be more convenient than that in [1], assumes that the mean stress and mean strain are in a linear relationship between and the relationship between the intensities of tangential stresses and shear strains depends on the stress mode.

The approach has been tested by analyzing specific processes of elastoplastic deformation of tubular specimens at constant and varying stress mode angles. The calculated axial and hoop components strains in these processes are in approximate agreement with experimental data.

The approach may be used to describe the elastoplastic deformation of a material when the strains do not exceed 7.5% and there is an insufficient number (less than three) of given values of base functions (1.17) in the strain range of interest.

Unlike the approach [1], our approach disregards the experimental fact that the mean plastic strain is zero ($\varepsilon_0^{(p)} = 0$).

When used to describe the inelastic deformation of Kh18N10T material, the proposed constitutive equations, which allow for the stress mode, produce strains that, if greater than 7.5%, are in better agreement with experimental data than those obtained by the theory of deformation along small-curvature paths.

REFERENCES

1. M. E. Babeshko, Yu. N. Shevchenko, and N. N. Tormakhov, "Constitutive equations of elastoplastic isotropic materials that allow for the stress mode," *Int. Appl. Mech*., **45**, No. 11, 1189–1195 (2009).
2. A. A. Il'yushin, *Plasticity: Fundamentals of Plasticity Theory* [in Russian], Izd. AN SSSR, Moscow (1963).
3. L. M. Kachanov, *Fundamentals of Plasticity Theory* [in Russian], GTTL, Moscow (1956).
4. Yu. N. Shevchenko, M. E. Babeshko, and R. G. Terekhov, *Thermoviscoelastoplastic Processes of Combined Deformation of Structural Elements* [in Russian], Naukova Dumka, Kyiv (1992).
5. Yu. N. Shevchenko and R. G. Terekhov, *Constitutive Equations of Thermoviscoplasticity* [in Russian], Naukova Dumka, Kyiv (1982).
6. M. E. Babeshko and Yu. N. Shevchenko, "Elastoplastic stress–strain state of flexible layered shells made of isotropic and transversely isotropic materials with different moduli and subjected to axisymmetric loading," *Int. Appl. Mech*., **43**, No. 11, 1208–1217 (2007).
7. M. E. Babeshko and Yu. N. Shevchenko, "On two approaches to determining the axisymmetric elastoplastic stress-strain state of laminated shells made of isotropic and transversely isotropic bimodulus materials," *Int. Appl. Mech*., **44**, No. 6, 644–652 (2008).
8. A. Z. Galishin, "Axisymmetric thermoviscoelastic state of thin flexible shells with damages," *Int. Appl. Mech*., **44**, No. 2, 158–166 (2008).
9. A. Z. Galishin, "Axisymmetric thermoviscoelastic state of thin laminated shells made of a damageable material," *Int. Appl. Mech*., **44**, No. 4, 431–441 (2008).
10. Yu. N. Shevchenko, R. G. Terekhov, and N. N. Tormakhov, "Constitutive equations for describing the elastoplastic deformation of elements of a body along small-curvature paths in view of the stress mode," *Int. Appl. Mech*., **42**, No. 4, 421–430 (2006).
11. Yu. N. Shevchenko, R. G. Terekhov, and N. N. Tormakhov, "Linear relationship between the first invariants of the stress and strain tensors in theories of plasticity with strain hardening," *Int. Appl. Mech*., **43**, No. 3, 291–302 (2007).
12. Yu. N. Shevchenko, R. G. Terekhov, and N. N. Tormakhov, "Elastoplastic deformation of elements of an isotropic solid along paths of small curvature: Constitutive equations incorporating the stress mode," *Int. Appl. Mech*., **43**, No. 6, 621–630 (2007).
13. M. Zyczkowski, *Combined Loadings in the Theory of Plasticity*, PWN, Warsaw (1981).